

Paper

Int'l J. of Aeronautical & Space Sci. 16(4), 581–589 (2015)
DOI: <http://dx.doi.org/10.5139/IJASS.2015.16.4.581>

IJASS
International Journal of
Aeronautical and Space Sciences

Monocular Vision-Based Guidance and Control for a Formation Flight

Bong-kyu Cheon*, **Jeong-ho Kim****, **Chan-oh Min****, **Dong-in Han****, **Kyeum-rae Cho***** and **Dae-woo Lee******

Department of Aerospace Engineering, Pusan National University, Pusan 46241, Republic of Korea

kie-jeong Seong*****

Korea Aerospace Research institute, Daejeon 34133, Republic of Korea

Abstract

This paper describes a monocular vision-based formation flight technology using two fixed wing unmanned aerial vehicles. To measuring relative position and attitude of a leader aircraft, a monocular camera installed in the front of the follower aircraft captures an image of the leader, and position and attitude are measured from the image using the KLT feature point tracker and POSIT algorithm. To verify the feasibility of this vision processing algorithm, a field test was performed using two light sports aircraft, and our experimental results show that the proposed monocular vision-based measurement algorithm is feasible. Performance verification for the proposed formation flight technology was carried out using the X-Plane flight simulator. The formation flight simulation system consists of two PCs playing the role of leader and follower. When the leader flies by the command of user, the follower aircraft tracks the leader by designed guidance and a PI control law, and all the information about leader was measured using monocular vision. This simulation shows that guidance using relative attitude information tracks the leader aircraft better than not using attitude information. This simulation shows absolute average errors for the relative position as follows: X-axis: 2.88 m, Y-axis: 2.09 m, and Z-axis: 0.44 m.

Key words: Vision-based formation flight, UAV, Position estimation, Attitude estimation, X-Plane, Light sport aircraft.

Nomenclature

h	Displacement of feature point between two frames.	fl	Focal length.
E	Estimation error.	V	Velocity, [m/sec].
F_f	Coordinates of feature point in the previous frame.	p, q, r	Roll/ Pitch/ Yaw rate, [rad/sec].
G_f	Coordinates of feature point in the current frame.	ϕ, θ, ψ	Roll/ Pitch/ Yaw angle, [rad/sec].
G_p	2-D projection plane of 3-D point.	δ	Deflection of control surface, [rad].
K_p	Parallel plane to G_p .	L	Leader plane.
w	Weighting function.	F	Follower plane.
M	Coordinates of 3-D model.	β	Sideslip angle, [rad].
m	Projection of M onto 2-D plane.	γ	Flight path angle, [rad].
P_i	Orthogonal projection of model plant.	H	Altitude, [m].
p_i	Projection of P_i onto image plane.	f	Forward direction distance, [m].
		l	Lateral direction distance, [m].
		K	Proportional gain.

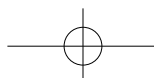
This is an Open Access article distributed under the terms of the Creative Commons Attribution Non-Commercial License (<http://creativecommons.org/licenses/by-nc/3.0/>) which permits unrestricted non-commercial use, distribution, and reproduction in any medium, provided the original work is properly cited.

© * Master's degree candidate
** Ph.D candidate
*** Professor
**** Professor, Corresponding author: baenggi@pusan.ac.kr
***** principal researcher

Received: June 22, 2015 Revised: October 20, 2015 Accepted: October 21, 2015
Copyright © The Korean Society for Aeronautical & Space Sciences

581

<http://ijass.org> pISSN: 2093-274x eISSN: 2093-2480



Subscripts

CMD	Command
rel	Relative
k	Keeping distance
d	Desired
th	Throttle
a	Aileron
e	Elevator
r	Rudder

1. Introduction

As unmanned aerial vehicle (UAV) applications have expanded from reconnaissance, search and rescue (SAR) operations, and parcel delivery to prompt strike attacker, many studies of formation flight of UAVs have been carried out. Recently, UAV formation flight missions, such as UAV swarm, have been researched widely. In order to reduce the fuel consumption rate by upwash generated from the wing tip vortex of the leader UAV, the formation flight of UAVs has received much attention as an essential technology.

Many studies about the control and guidance of multiple UAVs have been conducted. These studies include a formation flight experiment with UAVs utilizing bi-directional communication, and a guidance system utilizing relative velocity, attitude, and the position of the leader [1–8]. Sending and receiving its own position and attitude data through communication between the leader and follower and use the relative values. The conventional method can be easily jammed in enemy airspace if flight information is intercepted or the signal itself is jammed, resulting a breakup of the formation.

To overcome the problem related to communication loss, we propose an estimation algorithm utilizing feature points and an on-board monocular camera.

Similar vision-based formation flight studies have used the estimated relative position of the leader only. In [9], the subtended angle in an image related to the wingspan of the aircraft was measured. This data was compared with the actual wingspan of the aircraft and the estimated relative position was determined. These methods, however, have the limitation that the subtended angle can be altered by the attitude change of the leader. Another study measured an attitude of the leader with multiple infrared (IR) light-emitting diodes (LEDs). This method has the shortcoming that the infrared LEDs must be attached at the wing tips, elevator, and vertical stabilizer [10]. Other similar studies about operating UAVs in a jamming environment have been

carried out [11].

The proposed monocular vision-based formation flight algorithm features a guidance and control law using the relative position and attitude, which are obtained from the image of the leader only. This image processing technology is based on a description given in our previous paper [12], including a method of extracting feature points of fixed wing aircraft from an image without any attached markers and a method for estimating the relative position and attitude of a leader aircraft. In (12), we show the feasibility of a monocular vision-based measurement system using X-plane flight simulation commercial software.

In the present study, this paper considered the feasibility of monocular vision-based formation flight, including guidance and control, using the image processing algorithm described in [12]. The main contributions of this paper are that the measurement of position and attitude using a real formation flight image of two light sport aircraft (LSA) is presented for the verification of future real applications, and simulation including GNC using X-plane is presented for the verification of performance of formation flight by vision only. After measuring data from the leader aircraft, guidance and control command is generated. Follower aircraft in a real flight experiment cannot be controlled by the command. Thus, X-plane was adapted to verify G&C performance in this study.

In Section 2, we describe the feature point extraction method using images. The feature points are used to measure the relative position and attitude of the leader. Then, the relative position and attitude is used to estimate the position and attitude of the leader. The results of field flight tests using the LSA are used to verify the performance of the proposed vision-based system for the estimation of position and attitude. In Section 3, we describe the simulation environment, including parameter identification for the target airplane on the X-plane simulator, and the design of guidance and control laws. We also show the performance of the vision-based formation system for UAV using the X-Plane simulator. In Section 4, we give our conclusions for this study, and suggest improvements for vision-based formation flight.

2. Estimation of Position and Attitude for the Leader using Real Flight Images

2.1 State measurement of the leader

The KLT method and POSIT method are well-known algorithms that are used to measure the state of a target using monocular vision, Verified feasible results of real flight

In Fig. 3, M_x corresponds to a point on the 3-D model, and m_x is a projection of M_x onto the 2-D image plane. If the plane K_p is parallel to image plane G_p , P_i is a projection of model point M_i , which is orthogonal to the plane K_p . A projection of P_i onto the image plane is denoted as p_i . Also, N_i is a projection of model point M_i onto the plane K_p . u, v, w are the axes of the target frame, and x, y, z are the axes of the camera frame. i, j, k is the unit vector of each axis. fl represents the focal length of the lens. C is the center point of the image plane G_p .

The POSIT algorithm is based on POS (Pose from Orthography and Scaling). POS calculates the object-matrix using M_i . Then, the rotation matrix is derived by the previous object matrix and m_i , which is shown in image. The translation can be calculated by normalizing the first and second row of the rotation matrix as follows:

$$(M_0 - M_i) \times (fl / Z_0) i = x_i (1 + \varepsilon_i) - x_0 \tag{6}$$

$$(M_0 - M_i) \times (fl / Z_0) j = y_i (1 + \varepsilon_i) - y_0 \tag{7}$$

$$\varepsilon_i = (1 / Z_0) M_0 M_i \times k \tag{8}$$

In general, four to five iterations are required to calculate an optimum value of ε .

2.2 Verification of estimation method for the leader's position and attitude

2.2.1 Relative position measurement

A formation flight test using the LSA was carried out in order to obtain real images. In this test, a GPS and AHRS are installed on the leader. The fixed camera, GPS, and AHRS are installed on the follower. A laptop was used to record data and monitor the status. We can obtain the video images of the leader from formation flight. Then, the flight information



Fig. 4. Equipment used in experiment.



Fig. 5. Light sport aircraft (LSA) CTSW.

of the leader was obtained by the aforementioned relative distance and attitude estimation method. The construction of the equipment and the LSA (CTSWS) used in the flight experiment are shown in Figs. 4 and 5, respectively. Table 1 shows the specifications of the CTSW.

As shown by the flight trajectory in Fig. 6, the two aircraft tried to maintain a nearly constant distance during the flight. Figs. 7-9 show that the relative distances obtained from the monocular vision-based system are very similar to the GPS data. The mean square error with respect to the obtained GPS data is 1.050%, as shown in Eq. (9), with a standard deviation of 0.023%.

Table 1. Light aircraft specifications

Area, m ²	
Wing	9.98
Stabilator	1.65
Vertical tail	1.32
Wing span, m	8.53

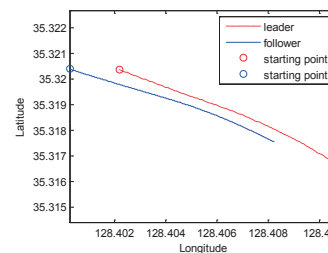


Fig. 6. Formation flight trajectory.

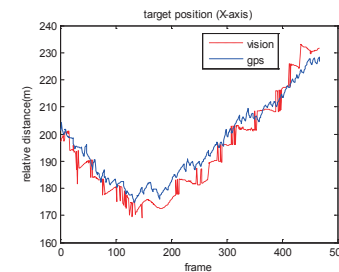


Fig. 7. X-axis relative distance.

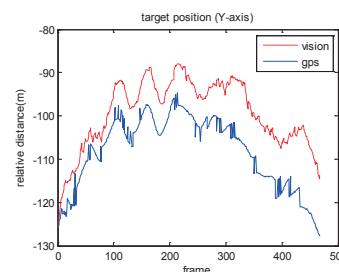


Fig. 8. Y-axis relative distance.

$$\left| \frac{rel_position_{GPS} - rel_position_{Vision}}{rel_position_{GPS}} \times 100(\%) \right| \quad (9)$$

Table 2 presents the quantitative analysis results for each axis. The relative distance error on the Y-axis is bigger than the same errors on the X and Z axes, according to a disturbance on the rolling axis from atmospheric air conditions.

In Figs. 7-9, significant chattering caused a large standard deviation. The first problem is the irregular time step of GPS logged data. The GPS position of the leader and follower

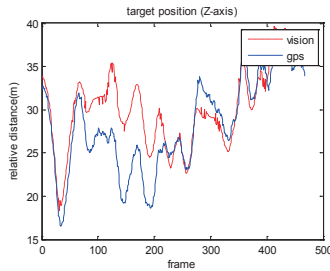


Fig. 9. Z-axis relative distance.

Table 2. Relative coordinate measurement results and error

	X-axis	Y-axis	Z-axis	Relative distance
Average error (m)	4.3978	8.8795	2.8914	3.8191
Standard deviation	2.4202	3.6482	2.4586	3.7419
Ratio of error	0.0226	0.0901	0.1155	0.0165

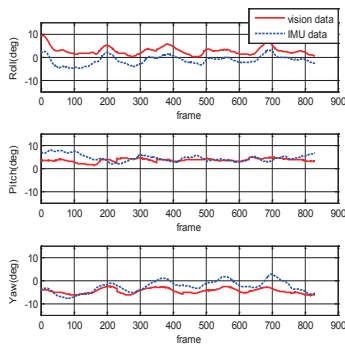


Fig. 10. Performance validation results for field formation flight.

Table 3. Performance validation results (straight flight path)

	X-axis	Y-axis	Z-axis	Relative distance
Average error (m)	4.3978	8.8795	2.8914	3.8191
Standard deviation	2.4202	3.6482	2.4586	3.7419
Ratio of error	0.0226	0.0901	0.1155	0.0165

were logged irregularly on two PCs, and this irregular time step caused chatter in the GPS data. Second, the camera was not rigidly mounted on the wing. Vibration from the aircraft affected the camera produced a large amount of chattering. If these problems are mitigated, the standard deviation of the results can be reduced.

2.2.2 Relative attitude measurement

Figure 10 shows the vision-based attitude measurement results for each axis. Table 3 shows the results of the video of 830 frames for 30 fps images. There is an average error of 4.0° and a standard deviation of 1.2° for the roll axis; an average error of 1.4° and a standard deviation of 1.3° for the pitch axis; and an average error of 2.1° and standard deviation of 1.4° for the yaw axis.

3. Simulation of Formation Flight System using X-Plane

3.1 UAV system modeling

This section shows the applicable availability of formation flight system using the X-plane simulator.

The RQ-101 “Song-Goal-Mae” was selected as the UAV model for simulation. Fig. 11 shows the configuration of RQ-101. The RQ-101 is currently used as a corps-level UAV in the military of the Republic of Korea (ROK). A model can be designed using the Plane Maker software of X-Plane[15] according to specifications given in Table 4.

Mathematical modeling for the follower is necessary to design the controller for leader tracking. In general, the mathematical modeling can be obtained from specifications and material properties. However, since accurate specifications of the RQ-101 are not known, the control inputs (δ_{th} , δ_e , δ_a , and δ_r) and system outputs (V , q , p , and



Fig. 11. RQ-101.

Table 4 RQ-101 Specifications

Weight	215 kg
Cruise speed	150 km/h
Length	4.57 m
Wingspan	6.4 m

r) were used to obtain the transfer function of the follower. In other words, an inverse method was used to obtain the modeling. To extract the values of control input and system output from X-Plane, we utilized an autopilot function of X-Plane to obtain flight data according to the change of velocity and roll/pitch/yaw angles while maintaining a constant altitude. The velocity, pitch rate, roll rate, and yaw rate transfer functions obtained using the results of the flight simulation are given in Eqs. (10), (11), (12), and (13), respectively.

$$\frac{V}{\delta_h} = \frac{3.153s + 0.04062}{s^2 + 0.05732s + 0.0004946} \quad (10)$$

$$\frac{q}{\delta_e} = \frac{13.82s + 72.6}{s^2 + 7.549s + 51.63} \quad (11)$$

$$\frac{p}{\delta_a} = \frac{32.32s + 9.189}{s^2 + 10.83 + 2.189} \quad (12)$$

$$\frac{r}{\delta_r} = \frac{0.0003267s + 3.91e-8}{s^2 + 0.0005801s + 2.487e-6} \quad (13)$$

3.2 Guidance law using relative distance and attitude for the follower

A guidance law for a formation flight can be separately designed in the lateral-directional and longitudinal directions. The geometric relationship of the formation flight in the lateral-directional aspect is shown in Eqs. (14) and (15):

$$f_x = (x_L - x_F), \quad l_y = (y_L - y_F) \quad (14)$$

$$\begin{bmatrix} l \\ f \end{bmatrix} = \begin{bmatrix} \sin \psi_L & -\cos \psi_L \\ \cos \psi_L & \sin \psi_L \end{bmatrix} \begin{bmatrix} f_x \\ l_y \end{bmatrix} \quad (15)$$

Position commands (shown as Eq. (16)) for formation flight are obtained using the difference between the desired position (Fig. 12) and the relative position. To minimize the difference of the heading angle between the leader and follower, the follower's azimuth ψ_F is controlled by ψ_{FCMD} as shown in Eq. (17).

$$y_d = \begin{bmatrix} l_d \\ f_d \end{bmatrix} \quad (16)$$

where $l_d = l - l_k$, $f_d = f - f_k$

$$\psi_{FCMD} = \psi_F + \tan^{-1} \frac{l_d}{f_d} \quad (17)$$

The guidance law of a follower that relies solely on relative position with respect to the leader has good performance in a straight flight path. However, in the case of a circular trajectory, the response time may be late because the

follower has a transient response. The roll angle of the leader, which is obtained from an image, is fed forward to ϕ_{FCMD} for efficiency and accuracy of guidance [2], as shown by Eq. (18):

$$\phi_{FCMD} = K_\psi e_\psi + K_{\phi_L} \phi_L \quad (18)$$

where e_ψ represents the angle of error between the follower's heading angle command (ψ_{FCMD}) and the follower's heading angle (ψ_F): ($\psi_{FCMD} - \psi_F$). ϕ_L and K_{ϕ_L} are the leader's roll angle and the proportional gain for roll, respectively.

The guidance law for the longitudinal directions can be determined by the difference in altitude between the leader and follower, as shown by Eq. (19):

$$H_{FCMD} = H_k + H_L \quad (19)$$

To maintain formation of the x-axis, the velocity command is obtained using the forward direction distance command as shown in Eq. (20):

$$V_{FCMD} = f_d K_{x_{rel}} + V_L \quad (20)$$

3.3 Performance evaluation using X-Plane simulation

3.3.1 X-Plane simulation environment

The simulation system requires two PCs to describe a formation flight experiment. In the Leader PC, X-Plane flight simulation software is executed and flight information is transferred to the Follower PC. The other X-Plane software is run on the follower PC. It receives the information and renders an image of the leader aircraft. Then, the rendered

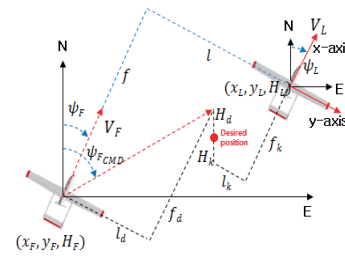


Fig. 12. Geometric relationship of formation.

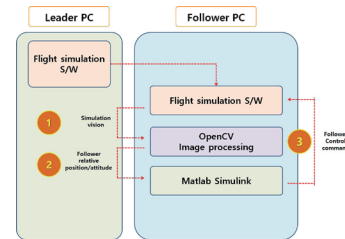


Fig. 13. Simulation program configuration.

scene is obtained using a frame grabber installed on the follower PC.

The positions of feature points extracted from the image are sent to Simulink via UDP communication. These feature points of 2-D coordinates are then processed to estimate relative position and orientation data, and these data are used for the guidance and controller block. Finally, the resulting control commands are passed to the X-Plane simulator via UDP communication [17]. Control surfaces of the follower aircraft are controlled according to the transferred control command input.

3.3.2 Application for video processing method in X-Plane simulation

Figure 14 shows the extraction of feature points, and the tracking area of the leader, in real time. The distinguishing feature points of the leader are extracted after looking in the area of the leader. By limiting the region of interest in which calculations are to be performed, the processing speed can be increased. The positional information for the feature points is transmitted into the Simulink block by UDP communication. This position information is used to determine the relative position and attitude of the leader. The resolution of the leader's image in simulation is 1920 by 1080. The processing time is 33 ms for the third generation i7 processor, and 50 ms for a mobile third generation i5 processor.

3.3.3 Results for the relative position and attitude estimation in X-Plane

This simulation was carried out reference to [12]. The

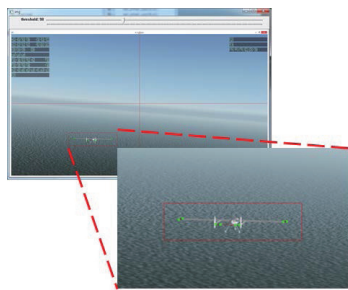


Fig. 14. Results for area and feature point extraction of the leader (wing tip dots).

Table 5. Mean and STD of position

	X-axis	Y-axis	Z-axis
Average Absolute error (m)	3.09	1.60	0.34
Standard deviation	2.14	2.86	0.70

relative position estimation uses two UAVs, wherein they are flown apart by -55 m, 6 m, and -6 m (corresponding to the X, Y, and Z axial distance of the body frame, respectively) to represent formation flight. The leader performs a maneuver to position itself from right to left, and then right again in the image of the follower.

Average errors and STDs of relative position are shown in Table 5.

The relative attitude estimation was performed under the same conditions as position estimation experience. The roll value changes from -8° to 8° when a left-to-right maneuver was performed, corresponding to reference data received with an error of around 1° . Due to the aliasing effect of 3-D graphics, oscillation of the orientation occurred in the simulation image, and it is larger than the results from real flight. Average errors and STDs are shown in Table 6.

3.3.4 Results for vision-based formation flight in X-Plane

To validate the developed formation flight system, formation flight is performed using X-Plane simulation. The test system is comprised of two PCs. One PC is used as the leader by using an embedded autopilot function of X-Plane to maintain altitude with heading change on demand. Then, an image of the leader is acquired by the follower's screen, which measures relative position and attitude to maintain formation flight. The image processing algorithm takes under 50 ms; thus, a control command can be generated up to 20 times per second, and flight data are saved at a corresponding rate of 20 Hz. Fig. 15 shows the flight path of the formation flight.

The formation flight simulation was carried out using two types of roll command. One is computed by using only the

Table 6. Mean and STD of attitude

	Roll	Pitch	Yaw
Average Absolute error ($^\circ$)	1.89	0.78	2.00
Standard deviation	3.19	1.54	2.56

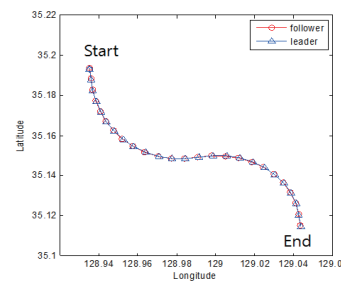


Fig. 15. Formation flight trajectory using optical sensor.

position data. The other is computed using the position data and leader's roll angle feedforward as described by Eq. (18).

To compare performance between adding roll angle feedforward and using only position information, the formation flight test maintained consistent distances of -55 m, 6 m, and -6 m for the X (front), Y (right), and Z (downward) axes, respectively, and was performed in X-Plane. The simulation was carried out under the same conditions as those of the leader (trajectory and velocity).

The follower can perform without any problems about the X-axis (Figs. 16 and 19) and Z-axis (Figs. 18 and 21). When the leader flights in a circle, a follower using attitude compensation can fly in a circle properly (Fig. 20). However, without using the leader's roll angle feedforward, considerable error occurs (Fig. 17).

With reference to Tables 7 and 8, the performance of formation flight using the only position data and using the leader's roll angle feedforward can be compared to the average of and the STD of the relative distance error.

4. Conclusion

This paper describes a monocular vision-based formation flight technology differentiated from the previous researches by measuring relative attitude information from the vision and using guidance law considering roll angle of the leader aircraft. From the captured image of the leader, feature points were extracted by KLT feature tracker and relative position and attitude of the leader were obtained from the POSIT algorithm. The proposed vision processing algorithm was verified through the field experiment using two light sport aircrafts and the algorithm took less than 50ms for each frame on a second generation i5 mobile CPU. To verify

Table 7. Mean and STD w/o roll feedforward

	X-axis	Y-axis	Z-axis
Average Absolute error (m)	2.23	6.93	0.37
Standard deviation	2.89	7.35	0.67

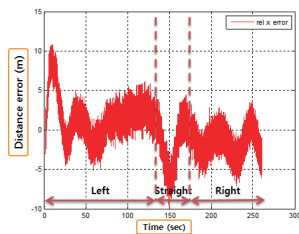


Fig. 16. Error for relative distance w/o roll feedforward (X-axis).

the performance of the guidance and controller, a formation flight simulator consisted of two PCs was setup. All the video data was processed on the follower PC. The control command was transmitted to the flight simulation S/W through UDP

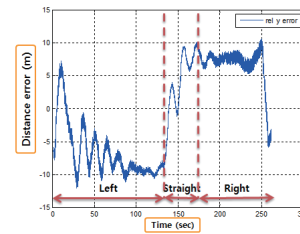


Fig. 17. Error for relative distance w/o roll feedforward (Y-axis).

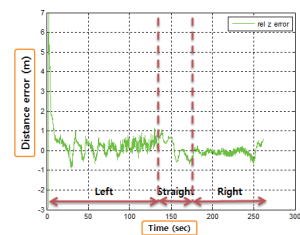


Fig. 18. Error for relative distance w/o roll feedforward (Z-axis).

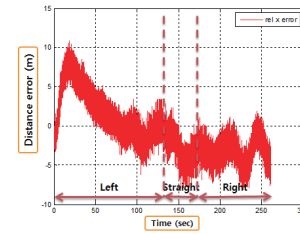


Fig. 19. Error for relative distance with roll feedforward (X-axis).

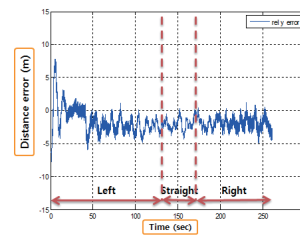


Fig. 20. Error for relative distance with roll feedforward (Y-axis).

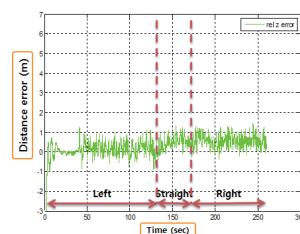


Fig. 21. Error for relative distance with roll feedforward (Z-axis).

Table 8. Mean and STD with roll feedforward

	X-axis	Y-axis	Z-axis
Average Absolute error (m)	2.88	2.09	0.44
Standard deviation	3.29	1.44	0.81

communication. Through this simulation, we verified that vision-based formation flight can be done without communication between the aircrafts. The formation flight position error was shown to be 2.88m less than 6.93m by considering the roll angle during guidance, when the leader was flying 60m away in front of the follower.

Acknowledgement

This research was supported by the Technology Innovation Program funded by the Ministry of Trade, Industry & Energy(MI, Korea) (grant number 10054930)

References

- [1] Yu Gu, Brad Seanor, Giampiero Campa, Marcello R. Napolitano, Larry Rowe, Srikanth Gururajan, and Sheng Wan "Design and Flight Testing Evaluation of Formation Control Laws," *IEEE TRANSACTIONS ON CONTROL SYSTEMS TECHNOLOGY*, Vol. 14, No. 6, November, 2006, pp. 1105-1112.
- [2] Yong-kyu Song, Chang-hwan Heo, Sang-jun Lee, and Jung-han Kim, "Autonomous Formation Flight Tests of Multiple UAVs," *Journal of The Korean Society for Aeronautical & Space Sciences*, Vol. 38 No. 3, March, 2010, pp. 264-273.
- [3] Dong-Il You, and Hyun-chul Shim, "Leader-Follower based Formation Guidance Law and Autonomous Formation Flight Test of Multiple MAVs," *Journal of The Korean Society for Aeronautical & Space Sciences*, Vol. 39, No. 2, February, 2011, pp. 121-127.
- [4] Hyo-Sang Shin, Min-Jea Thak, and Hyoun-Jin Kim, "Nonlinear Model Predictive Control for Multiple UAVs Formation Using Passive Sensing," *International Journal of Aeronautical and Space Sciences*, Vol. 12, No. 1, 2011, pp. 16-23.
- [5] Yoichi Sato, Takeshi Yamasaki, Hiroyuki Takano, and Yoriaki Baba, "Trajectory Guidance and Control for a Small UAV," *KSAS International Journal*, Vol. 7, No. 2, November, 2006, pp. 137-144.
- [6] Jongug Choi, and Youdan Kim, "UAV Formation Flight Control Law Utilizing Energy Maneuverability," *KSAS International Journal*, Vol. 9, No. 1, May, 2008, pp. 31-41.
- [7] Mingu Kim, and Youdan Kim, "Multiple UAVs Nonlinear Guidance Laws for Stationary Target Observation with Waypoint Incidence Angle Constraint," *International Journal of Aeronautical and Space Sciences*, Vol. 14, No. 1, 2013, pp. 67-74.
- [8] Jin-Wook Lee, and H. Jin Kim, "Waypoints Assignment and Trajectory Generation for Multi-UAV Systems," *KSAS International Journal*, Vol. 8, No. 2, November, 2007, pp. 107-120.
- [9] Seung-Min Oh, and Eric N. Johnson., "Relative Motion Estimation for Vision-based Formation Flight using Unscented Kalman Filter," *AIAA Guidance, Navigation and Control Conference and Exhibit*, Aug, 2007, pp. 20-23.
- [10] Zouhair Mahboubi, Zico Kolter, Tao Wang, Geoffrey Bower, and Andrew Y. Ng, "Camera Based Localization for Autonomous UAV Formation Flight," *Infotech@Aerospace Conference(AIAA)* 2011, March, 2011, pp. 1-13.
- [11] Youngjoo Kim, Wooyoung Jung and Hyochoong Bang, "Visual Target Tracking and Relative Navigation for Unmanned Aerial Vehicles in a GPS-Denied Environment," *International Journal of Aeronautical and Space Sciences*, Vol. 15, No. 3, 2014, pp. 258-266.
- [12] Jin-Woo Heo, Jeong-Ho Kim, Dong-In Han, Dae-Woo Lee, Kyeum-Rae Cho, and Gi-bong Hur., "Pose Estimation of Leader Aircraft for Vision-based Formation Flight," *Journal of The Korean Society for Aeronautical & Space Sciences*, Vo.41, No.7, July, 2013, pp.532-538.
- [13] Bruce D. Lucas, and Takeo Kanade, "An Iterative Image Registration Technique with an Application to Stereo Vision" *IJCAI'81 Proceedings of the 7th international joint conference on Artificial intelligence-Vol. 2*, 1981, pp. 674-679.
- [14] Carlo Tomasi, and Takeo Kanade, "Detection and Tracking of Point Features", Carnegie Mellon University Technical Report CMU-CS-91-132, April, 1991.
- [15] PlaneMaker manuals home page, "<http://developer.x-plane.com/manuals/planemaker/>".
- [16] Byung-soo Kim, You-dan Kim, Hyo-choong Bang, and Min-jea Tahk, Sung-kyung Hong, *Flight dynamics and control, fourth ed*, Kyungmoon, Seoul, 2004, Chapter 7, 8.
- [17] Young-jun Seo, Chan-oh Min and Dae-woo Lee, "Development and Flight Test of Auto-landing System Using X-Plane Simulator," *Proceedings of KSAS Fall Meeting*, April, 2011, pp. 435-440.